REPORT DOCUMENTATION PAGE

1. REPORT DATE *(DD-MM-YYYY)*	2. REPORT TYPE	3. DATES COVERED *(From - To)*

4. TITLE AND SUBTITLE

5a. CONTRACT NUMBER

5b. GRANT NUMBER

5c. PROGRAM ELEMENT NUMBER

6. AUTHOR(S)

5d. PROJECT NUMBER

5e. TASK NUMBER

5f. WORK UNIT NUMBER

7. PERFORMING ORGANIZATION NAME(S) AND ADDRESS(ES)

8. PERFORMING ORGANIZATION REPORT NUMBER

9. SPONSORING/MONITORING AGENCY NAME(S) AND ADDRESS(ES)

10. SPONSOR/MONITOR'S ACRONYM(S)

11. SPONSOR/MONITOR'S REPORT NUMBER(S)

12. DISTRIBUTION/AVAILABILITY STATEMENT

13. SUPPLEMENTARY NOTES

14. ABSTRACT

15. SUBJECT TERMS

16. SECURITY CLASSIFICATION OF:			17. LIMITATION OF ABSTRACT	18. NUMBER OF PAGES	19a. NAME OF RESPONSIBLE PERSON
a. REPORT	b. ABSTRACT	c. THIS PAGE			
					19b. TELEPHONE NUMBER *(Include area code)*

SWIR variable dispersion spectral imaging sensor

F. D. Shepherd, J. M. Mooney, T. E. Reeves, D. S. Franco, J. E. Murguia, C. Wong
P. Dumont, F. Khaghani, and G. Diaz

Solid State Scientific Corporation
Nashua, NH

M. M. Weeks and D. Leahy[1]

Air Force Research Laboratory
Hanscom AFB, MA

ABSTRACT

A novel spectral imaging sensor based on dual direct vision prisms is described. The prisms project a spectral image onto the focal plane array of an infrared camera. The prism set is rotated on the camera axis and the resulting spectral information is extracted as an image cube (x, y, λ), using tomographic techniques. The sensor resolves more than 40 spectral bands (channels) at wavelengths between 1.2 μm and 2.5 μm wavelength. The sensor dispersion characteristic is determined by the vector sum of the dispersions of the two prisms. The number of resolved channels, and the related signal strength per channel, varies with the angle between the prism dispersion axes. This is a new capability for this class of spectral imaging sensor. Reconstructed short-wave imagery and spectral data is presented for field and laboratory scenes and for standard test sources.

Key Words: spectral imaging, short wavelength infrared, variable dispersion

1. INTRODUCTION

Mooney described the Chromotomographic Hyperspectral Imaging Sensor (CTHIS) in 1995[2]. In this type of sensor, a scene is observed through a telescope, having a field stop of known optical and surface properties, as shown in Figure 1. The object scene is imaged at the sensor field stop and re-imaged at the focal plane of the infrared (IR) camera. The resulting camera image includes the external scene framed by the focused field stop. Sensor calibration includes image information from the field stop. A Direct Vision Prism (DVP) disperses light.[3] This prism is mounted on the sensor optical axis, between the telescope and camera. The image at the focal plane is blurred by dispersion along an axis, corresponding to the dispersion direction of the DVP. Rotating the prism and the dispersion-axis of the image multiplexes color information. Two-dimensional image frames are collected as the prism rotates. These frames are input to image processing similar to Computer Aided Tomography to reconstruct a three-dimensional image cube, of dimensions (x, y and λ). Selection of any pixel in the xy-plane of the cube, gives the spectrum emitted and / or reflected from the corresponding location in object space. CTHIS sensors have been demonstrated in the visible, mid-wave infrared (MWIR) and long-wave infrared (LWIR) spectral bands.

---

[1] Now with Air Force Electronic Systems Center, Hanscom AFB, MA.
[2] J. M. Mooney, "Angularly multiplexed spectral imager," Proc. SPIE, Vol. 2480, pp. 65-77, June, 1995.
[3] The Direct Vision Prism has at least two elements and zero net dispersion at a central wavelength. Shorter wavelengths are dispersed in one direction, along the dispersion axis, while longer wavelengths are dispersed in the opposite direction.
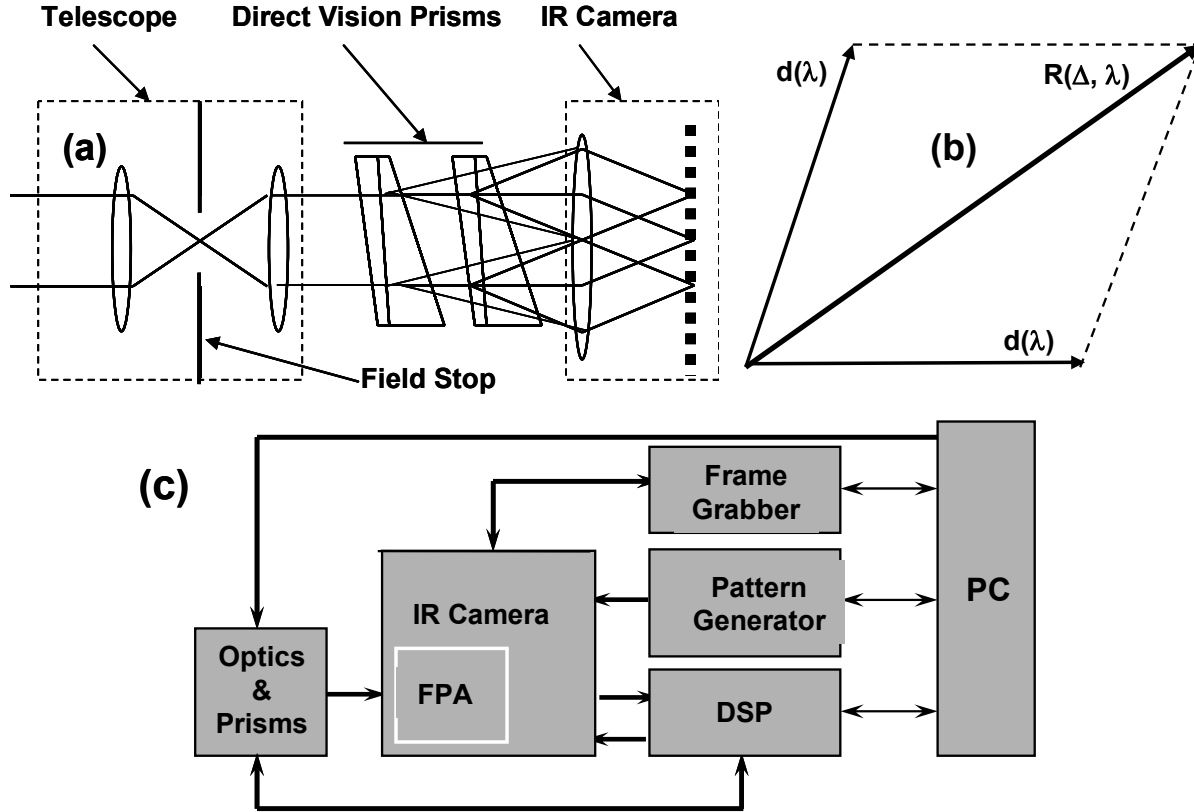
Figure 1: Schematic for variable dispersion SWIR spectral imaging sensor, including:
(a) the optics subsystem, (b) dispersion vector addition and (c) the system block diagram.

This paper reports a third generation CTHIS sensor, operating in the SWIR spectrum, between 1.1 μm and 2.5 μm, wavelength. The new sensor features variable dispersion, which is determined by the combined response of two direct vision prisms. A schematic of the sensor is seen in Figure 1. The sensor optics system was designed by Jon Mooney and the electro-mechanical system by Toby Reeves, co-authors of the current paper.

2. SENSOR OPERATION

Figure 2 is a photograph of the sensor optical subsystem with the cover removed. Referring to Fig. 1(a), each of the direct vision prisms is mounted in a rotary bearing, driven by a computer controlled stepping motor. The prisms are matched with respect to dispersion as a function of wavelength. The dispersion of each prism is described by a vector $d(\lambda)$. The prisms are rotated independently. The relative alignment of the two prism dispersion axes is described by an angle Δ, which varies from 0 to 2π. The resultant dispersion $R(\Delta,\lambda)$ is given by vector addition of the two prism dispersions:

$$R(\Delta, \lambda) = 2d(\lambda)\cos(\Delta/2) \tag{1}$$

Thus $R(\Delta, \lambda)$ varies from zero to twice the dispersion of the individual prisms. This variation is essentially continuous, as the stepping angle precision is $\pi/20,000$
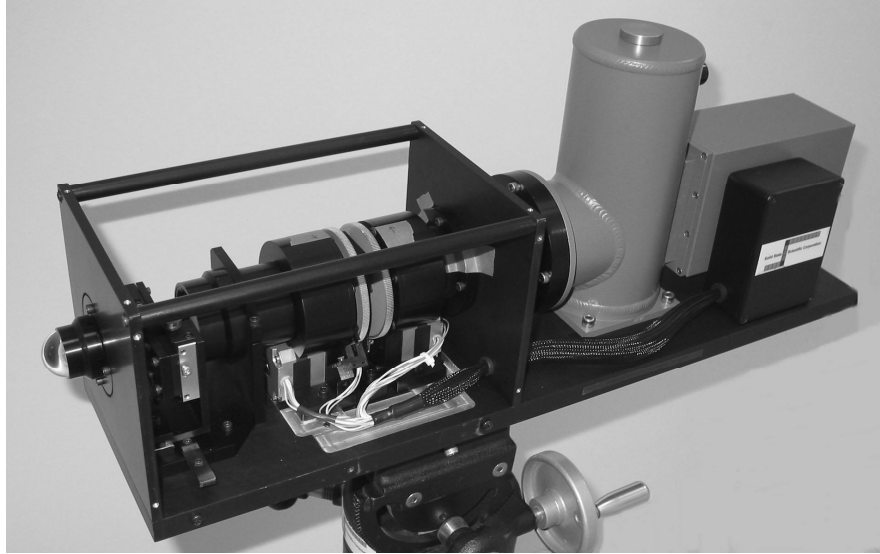
Figure 2: Sensor optics subsystem showing left to right, telescope with field stop,
dual direct vision prism mounts, camera optic and InSb SWIR camera/dewar.

3. MEASUREMENT OF VARIABLE DISPERSION

The sensor dispersion characteristic was evaluated by imaging the output of a grating monochromator, as the wavelength was advanced from 1.0 μm to 3.5 μm, in 0.01 μm steps. The sensor was synchronized with the monochromator to capture an image frame after each step. A normal, polychromatic, image of the monochromator port occurs at the sensor field stop. This image is re-imaged through the dual-direct vision prism, to form a spectral image at the focal plane. Given monochromatic illumination, the image at the focal plane is a shifted replica of the normal image. The magnitude of the image shift gives the relative sensor dispersion as a function of wavelength.

The focal plane response was pre-processed by scanning the array prior to illumination, to determine the location of "bad" pixels, those having signals more than 3-sigma from the mean. The response at "bad" pixel locations was replaced by the mean response of the array. Pre-processing reduced noise and extended both the dynamic range and the spectral range of the image shift measurement.

The measured shift of the spectral image with wavelength is given in Figure 3. Image shift is determined by detecting and tracking the location of the pixel having the maximum response in each frame. The use of the maximum response introduced discrete steps in the position, as the signal peak moved across pixel boundaries. This effect is apparent in the display of Figure 3. The actual image shift is continuous. A related measurement error, caused by an image tracing the boundary between two pixels, is apparent in the "0.00" trace. The expected result is zero for all wavelengths.

The relative prism angle, Δ was set at several angles to control sensor dispersion. The observed angles and dispersion reduction factor are given in Table 1. The reduction is uniform for all wavelengths.

Prism Angle Δ	0°	82.8°	120°	151°	180°
Dispersion Factor	1.00	0.75	0.50	0.25	0.00

Table 1: Reduction of sensor dispersion as a function of the angle between prism axes.
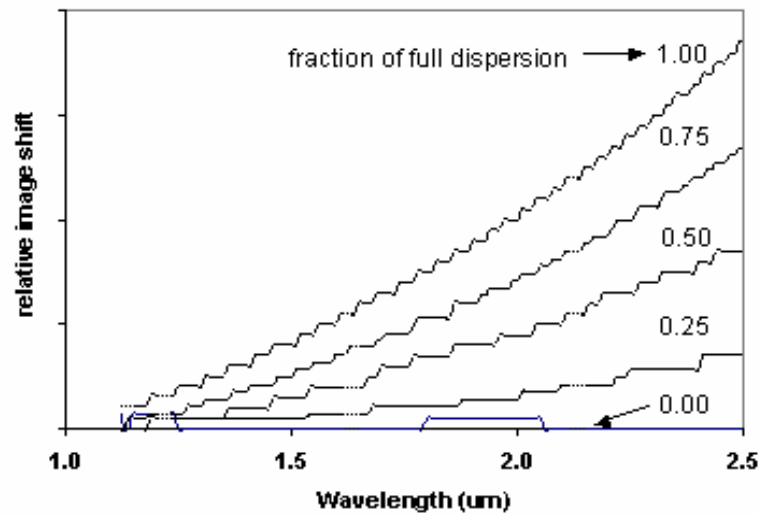
Figure 3: Image shift as a function of wavelength, for full and fractional dispersion

4. FIELD MEASUREMENTS

SWIR spinning prism image sets were taken during a day in June. Conditions included very light fog and some haze in low-lying areas. The visible range was estimated as 5 km. Image sets were processed using the method described by Mooney,[4] to obtain SWIR spectral image cubes. Each cube measured approximately 512 x 512 x 50 (wavelengths).

Figure 4 gives two cropped frames from reconstructed image data, taken while looking west at 10:00 AM. These images are typical of the better frames obtained. Other image frames display reduced contrast, the result of atmospheric or materials absorption. In the limit, images converge to gray, without discernable dynamic range. Some residual artifacts remain. Contrast is lost at short wavelengths, the result of absorption in a silicon component. Contrast also degrades at long wavelength, the result of the transmission losses in the short-pass filter. In each case image information is lost.
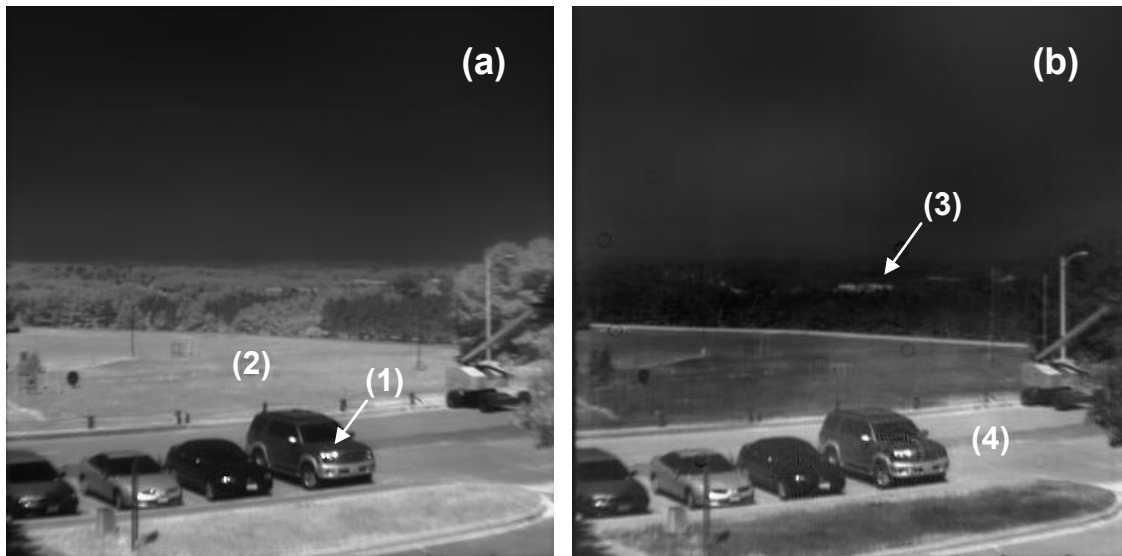

Figure 4: Reconstructed images of mid-morning sunlit scene with haze. (a) spectral-band 40, centered at 1.41 μm) and (b) spectral-band 21, centered at 2.01 μm.

---

[4] Mooney see Ref 2 above

Figure 5 gives the measured spectrum for 4 pixels from the same image cube utilized for Figure 4. The pixels are located at the glint from the right hand vehicle, the grassy area behind the vehicles, the distant building and the asphalt to the right of the vehicles.
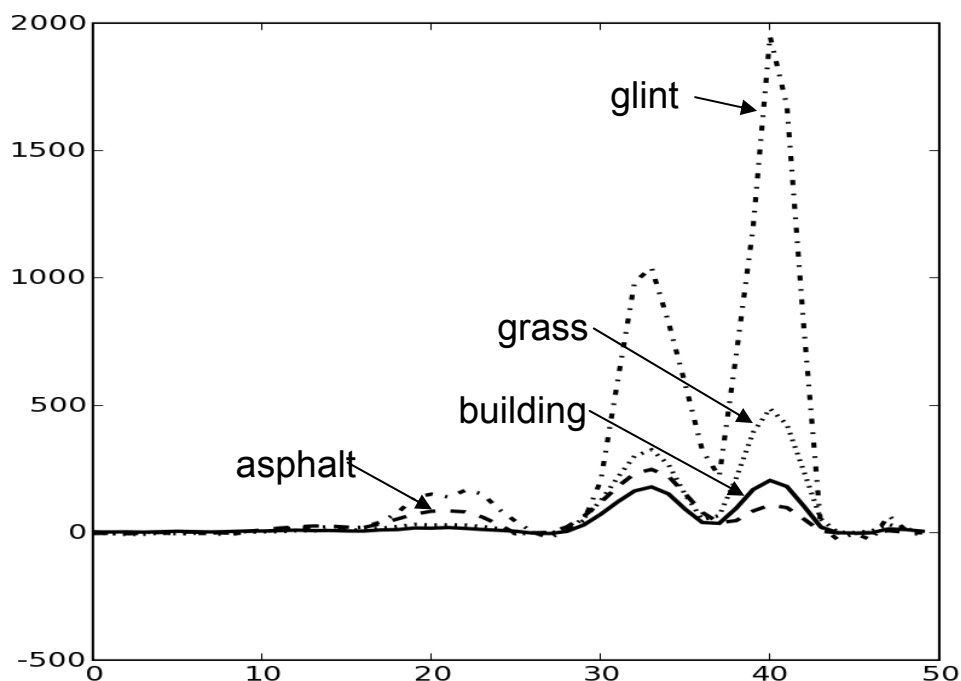

Figure 5: Spectra from four pixels from the image cube employed in Figure 4.

5. OBSERVATION OF LABORATORY SCENES

Figure 6 is the image of a laboratory scene including a blackbody source and controller, assembled with soda bottles and cans. The scene is front-illuminated with an incandescent lamp. Otherwise, the scene is generally dark, because the spectrum of fluorescent illumination is outside the measurement band.
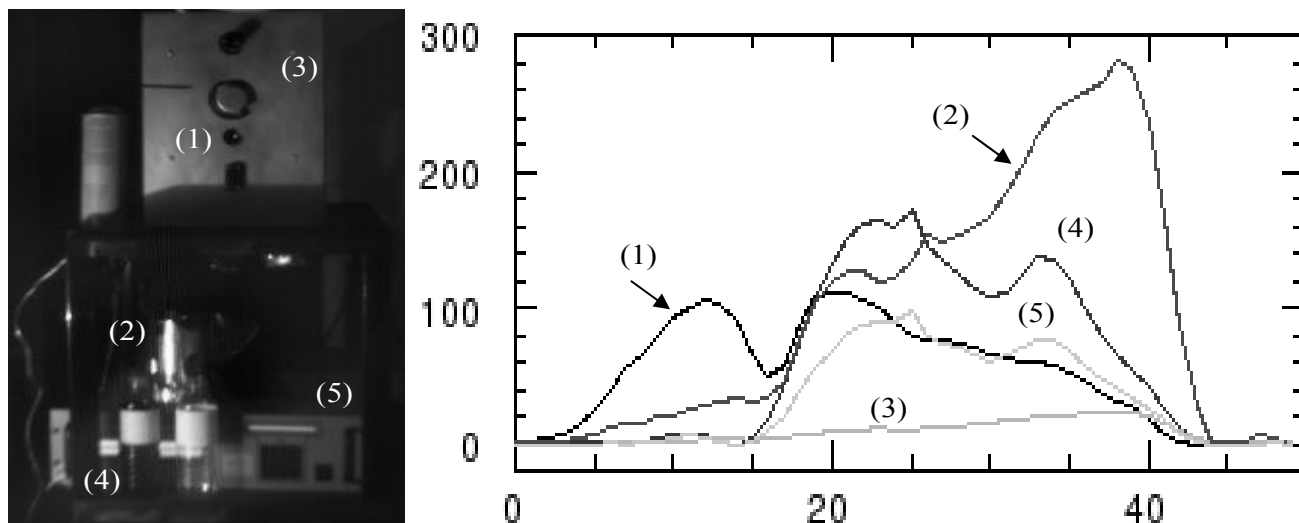

Figure 6: Components in blackbody measurement scene (1) emission from 800 C blackbody with 5 mm, sub-pixel aperture, (2) incandescent glint, (3) incandescent scatter, (4) emission from large panel display and (5) small panel display.

Figure 7(A) is a processed image of the 800 C blackbody aperture. Histogram projection[5] expands the image dynamic range, so as to display both weak and strong signals in the display. The display includes the direct image of the aperture (1) as well as two images that have been reflected and scattered from a whiteboard (2) and an asphalt tile floor (3). Figure 7(B) gives the logarithmic response for these three images. The signals span the full, 14-bit, dynamic range of the camera system. Note there is minimal change in signal spectrum, while the incident signal magnitudes change 100-fold.
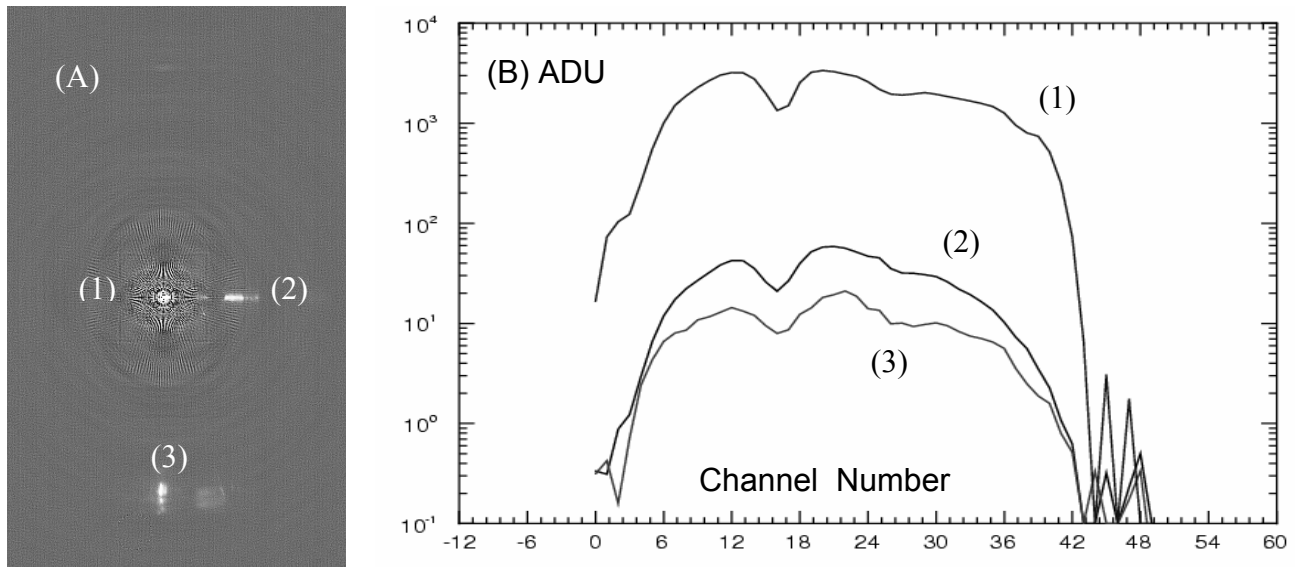

Figure 7: (A) Compressed image of 800 C blackbody aperture (1) with image reflected from white-board (2) and image scattered from asphalt tiles (3). (B) Logarithmic spectra for the same signals.

6. RESULTS AND CONCLUSIONS

A new short-wave infrared spectral imaging sensor is designed and demonstrated. The sensor is based upon the Chromotomographic Hyperspectral Imaging System reported by Mooney, Ewing and others[6]. However, the present sensor has variable spectral dispersion, allowing trade-off between signal strength and spectral resolution. The sensor operates in the SWIR spectral band between 1.2 μm and 2.5 μm wavelengths; where between 40 and 50 spectral bands are resolved. Spectral content is maintained over a wide range of incident signal intensity.

7. ACKNOWLEGEMENTS

---

[5] J. Silverman and V. E. Vickers, "Display and Enhancement of Infrared Images", Electro-Optical Displays, Edited by. Mohammad A. Karim, Marcel Dekker, Inc, New York, NY, 1992.
[6] J. M. Mooney, W.S. Ewing, et al., "High Throughput Hyperspectral Infrared Camera," J. Optical Society of America, A, Vol. 14, No. 11, November 1997.